Journal of Molecular Liquids 375 (2023) 121384

Contents lists available at ScienceDirect

Journal of Molecular Liquids

journal homepage: www.elsevier.com/locate/molliq

Effect of coating nanostructure on the electrokinetics of polyelectrolyte-coated particles. Grafted vs adsorbed polymer

S. Ahualli [a,b], S. Orozco-Barrera [a], A.L. Medina Castillo [c], A.V. Delgado [a,b,d,*]

[a] Departamento de Física Aplicada, Facultad de Ciencias, Spain
[b] MNat Unit of Excellence, Spain
[c] Departamento de Química Analítica, Spain
[d] Instituto de Investigación Biosanitaria IBS.GRANADA, Universidad de Granada, 18071 Granada, Spain

ARTICLE INFO

Article history:
Received 1 December 2022
Revised 27 January 2023
Accepted 1 February 2023
Available online 4 February 2023

Keywords:
Ac electrokinetics
Dielectric dispersion
Dynamic mobility
Grafted layer
Polyelectrolyte coating

ABSTRACT

In this work, the electrokinetic response of nanoparticles suspensions under the action of alternating electric fields is analyzed for the case that the particles are coated with a shell of polyelectrolyte. This is an important field of application of colloidal systems, as the coating is necessary or even unavoidable for control of the stability or functionalization of the particles for a specific use. Characterization of the coating in situ is not an easy task, and electrokinetics can help in answering this question, if one goes beyond the simple routine evaluation of the electrophoretic mobility of the particles, which will provide information on the sign (and perhaps a sort of effective amount) of the surface charge and potential, but little more. The richness and rigour of the information is much more significant if AC fields are used. This is the case for the techniques evaluated in the present investigation, namely, AC electrophoresis and dielectric dispersion. They jointly sweep several decades in frequency, and are sensitive in different manners to the size of the particles, the charge of the core and the shell, the thickness and rigidity of the latter, etc. In addition, an important distinction is made between coatings with a soft or adsorbed layer structure and those with a grafted, ideally radially arranged (brush-like) polyelectrolyte. A model is first described for the AC electrokinetics in both cases, and it is demonstrated that the brush structure magnifies the Maxwell-Wagner (or double layer) polarization, leading to an elevation in the AC mobility for frequencies around the MHz, and it very much raises the amplitude of the alpha- or concentration-polarization relaxation detected in the dielectric dispersion. The distribution of the charge in a thicker region for the brush structure explains these results. Experimental investigations are carried out with silica spheres coated by PDADMAC (+) and PSS (-) polyelectrolytes in the soft-layer case, and by (vinylbenzyl)trimethylammonium chloride (+) and sodium 4-vinylbenzenesulfonate (-) monomers that were polymerized (grafted) on the particles. The results show that the brush coating produces the expected MW elevation of the mobility, mostly in the case of the cationic polymer, apparently better attached to the particles by electrostatic attraction to the negative charge of the core silica particles. In contrast, a rather monotonous decrease of the mobility in absolute value is measured for the soft coatings, indicating that the inertia of the particles sets out at lower frequencies because of aggregation. Dielectric spectra confirm the better stability in the presence of the grafted polymer, although a low-frequency elevation in the logarithmic derivative of the permittivity is a proof of the existence of aggregates, less abundant in any case than for soft coatings. Dielectric data also confirm the different amounts of charge, larger for grafted cationic layers than for anionic ones. Finally, the model elaborated can fit the experimental results yielding quantitative values of the main parameters of the coated particles, namely, effective size, overall charge of the coating, and thickness and ionic permeability of the latter.

1. Introduction

There is a countless number of situations in which nanoparticles dispersed in a liquid medium need to be coated by one or more polymer layers. To mention just a few examples, consider first the biomedical field. The particles injected in the blood stream will be

* Corresponding autor at: Departamento de Física Aplicada, Facultad de Ciencias, Universidad de Granada, 18071 Granada, Spain.
E-mail address: adelgado@ugr.es (A.V. Delgado).

https://doi.org/10.1016/j.molliq.2023.121384
0167-7322/

very soon identified by macrophages and retired to the liver or spleen upon adsorption of plasma proteins known as opsonins [1–5]. The adsorption is minimized if some polymers are adsorbed on the particles prior to their injection; examples of these are poly (ethylenglycol) (PEG), dextran, or chitosan [6–8]. In addition, if the polymer is charged (polyelectrolyte), the overall charge of the particle can be controlled upon adsorption of the proper polymer. This has an obvious effect on the interactions between the nanoparticles and the opsonins or the cell membranes in the examples mentioned. Moreover, this also affects the particle–particle interactions and hence the physical stability of *dispersed* systems [9], a more general issue when working with such systems.

It is not immediately clear how to proceed with an efficient and long-lasting coating of the particles, generally known as *soft particles* when they possess that structure [10,11]. The most usual way is the procedure known as *layer-by-layer* deposition [12,13]: one [14–16] or more [17,18] layers are adsorbed by electrostatic interactions, either between the layer and the interface or between successive, oppositely charged layers. In the former case, the stability of the coating is not guaranteed, whereas in the latter multiple attractive interactions favor the stable presence of the last layer [19].

Previous works have demonstrated that the behaviour of polyelectrolyte-coated particles, as ascertained by electrokinetic techniques, can display unexpected features when the polymer is grafted rather than simply adsorbed on the particle: an extreme case is that of the so-called *polyelectrolyte brushes*. The polymer chains grow in a typically radial fashion producing a nanostructure in which the polyelectrolyte protrudes from the surface into the solution. For instance, it was found that the dynamic electrophoretic mobility (mobility in presence of ac electric fields in the MHz frequency range) was magnified for all frequencies, and the same applies to the amplitude of the dielectric dispersion (dependence of the dielectric constant of the suspension on the frequency of the field) [20,21].

In spite of these contributions, no systematic study has been performed comparing systems prepared by both methods, that is, adsorbed vs grafted polymer coatings. This is the objective of the present work: silica nanospheres will be coated by a negative polyelectrolyte (PSS, poly(styrene sulfonate)) or a positive one (PDADMAC, poly(diallyl dimethyl ammonium chloride)) using the standard adsorption method, starting from solutions of preformed polymers. The same particles will be functionalized in such a way that the respective monomer (sodium 4-vinylbenzene sulfonate in the case of the anionic polymer, and vinylbenzyl trimethylammonium chloride for the cationic one) polymerizes directly on the surface of the core particle, forming chains extending out of the latter. A comparison will be carried out between the electrokinetic behaviours of both kinds of systems in presence of alternating electric fields, for different volume fractions of particles and electrolyte concentrations in the medium.

2. Model

A nanoparticle coated with a polyelectrolyte layer can be envisioned as a hard sphere wrapped with a soft layer permeable to the ions and the liquid. Fig. 1 is a scheme of the *core/adsorbed layer* nanostructure. A polyelectrolyte shell with volume charge density ρ_{pol} and thickness L surrounds a spherical rigid core of radius R_C and surface charge density σ. A suspension of these particles contains a volume fraction of solids equal to ϕ and N types of ionic species with number concentrations (far from the particle) $n_i^0(\infty)$, charges ez_i, and diffusion coefficients D_i. The solution has a mass density equal to ρ_m, a viscosity η_m, and an electrical permittivity $\varepsilon_m\varepsilon_0$ (ε_0 is the vacuum permittivity). No restriction is imposed to the value of the volume fraction, and the finite concentration of particles is taken into account by using the so-called cell model: a single particle is considered dispersed in a concentric sphere of solution of radius b, the cell, in such way that $\phi = R_c^3/b^3$. The interactions (both electrostatic and hydrodynamic) are indirectly accounted for by proper setting of boundary conditions on the cell limit, $r = b$ (r is the radial spherical coordinate with origin at the particle center). The governing partial differential equations are well known:

i. Poisson-Boltzmann for ion concentration and electrical potential distributions both outside and inside the layer:

$$\begin{aligned}\nabla^2\Psi &= -\tfrac{1}{\varepsilon_m\varepsilon_0}\sum_{i=1}^{N} ez_i n_i, \quad r > R_C + L\\ \nabla^2\Psi &= -\tfrac{1}{\varepsilon_m\varepsilon_0}\sum_{i=1}^{N} ez_i n_i - \tfrac{\rho_{pol}}{\varepsilon_m\varepsilon_0} \quad R_C < r < R_C + L\end{aligned} \tag{1}$$

Here, k_B is Boltzmann's constant and T is the absolute temperature. Note that, because an alternating electric field will be applied, a dependence $(\boldsymbol{r}, t)$ is implicit in Ψ and the concentrations n_i.

ii. Navier-Stokes equations for incompressible fluid velocity $\mathbf{u}$ (with respect to the particle), again outside the layer and inside it:

$$\begin{aligned}\rho_m \tfrac{\partial \boldsymbol{u}}{\partial t} &= -\nabla P + \eta_m\nabla^2\boldsymbol{u} - \sum_{i=1}^{N} ez_i n_i \nabla\Psi, \quad r > R_C + L\\ \rho_m \tfrac{\partial \boldsymbol{u}}{\partial t} &= -\nabla P + \eta_m\nabla^2\boldsymbol{u} - \sum_{i=1}^{N} ez_i n_i \nabla\Psi - \gamma\boldsymbol{u}, \quad R_C < r < R_C + L\\ \nabla\cdot\boldsymbol{u} &= 0\end{aligned} \tag{2}$$

Here, P is the pressure, the term $-\gamma\boldsymbol{u}$ represents the extra friction between the fluid and the polyelectrolyte layer, and it is usually expressed in terms of the coefficient of permeability of the layer, λ (dimensions of reciprocal length), defined as [14]:

$$\lambda = \sqrt{\gamma/\eta_m} \tag{3}$$

iii. Nernst-Planck ionic conservation:

$$\begin{aligned}\tfrac{\partial n_i}{\partial t} + \nabla\cdot[n_i\boldsymbol{v}_i] &= 0\\ \boldsymbol{v}_i &= \boldsymbol{u} - \tfrac{D_i}{k_BT}\nabla\mu_i\end{aligned} \tag{4}$$

where the electrochemical potential of species i is given by:

$$\mu_i = \mu_i^* + ez_i\Psi + k_BT\ln n_i \tag{5}$$

μ_i^* being the reference potential.

We propose a model, described in the work of Ahualli et al. [21], which is a modification of that elaborated for soft particles with a polyelectrolyte shell. Eqs. (1–5) will be used as shown above, but they will be changed according to the following criteria. If, instead of the adsorbed nanostructure, a *grafted polyelectrolyte* is supposed to cover the core, one can imagine that the polymer chains will grow out from the surface $r = R_C$ in a radial fashion, as schematically depicted in Fig. 1. In this way, the polymer chain density will decay with $1/r^2$ and, therefore the charge density will decay with the same dependency:

$$\rho_{pol} = \frac{Q_{pol}}{4\pi L r^2} \tag{6}$$

This distribution will directly affect the fluid flow, which will be reduced by the stronger drag force where the polymer chains are more densely packed (close to the core surface). Assuming that

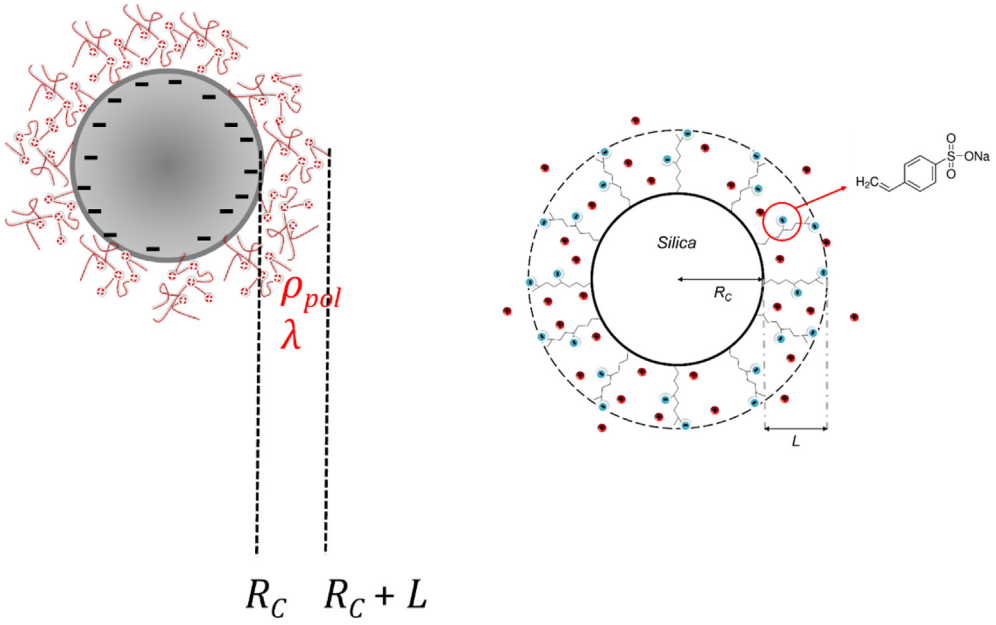

Fig. 1. Left: schematics of a spherical particle core of radius R_C coated with a layer of polyelectrolyte with charge density and thickness L. The friction coefficient of the layer is λ (see text for its definition). Right: representation of a rigid particle coated by a grafted anionic polyelectrolyte layer.

the friction sites are spherical and homogeneously distributed along the chains, and that they produce a Stokes friction, the polymer layer permeability will be reduced in the vicinity of the particle surface, and the friction parameter γ will have the same r^{-2} dependence as the chain density. From Eq. (3), one can obtain a decay for λ:

$$\lambda = \lambda_0 \frac{R_c}{r} \tag{7}$$

where the "0" subscript refers to the value used in the adsorbed layer model. Finally, the diffusion of ions also will be affected close to the interface, decreasing in the region with a high packing density and reaching the bulk value at the end of the polymer layer. It is logical to assume a radial dependence reciprocal to that of the chain distribution as follows:

$$D_i = D_{i0} \frac{r^2}{(R_C + L)^2} \tag{8}$$

where D_{i0} is the diffusion coefficient in the bulk.

As mentioned, an alternating electric field of frequency ω, $\boldsymbol{E}\exp(-j\omega t)$, is applied to the suspension to evaluate the dynamic electrophoretic mobility of the particles and the dielectric dispersion of the system. The field amplitude is small enough (but this includes any realistic field used in experiments) for the quantities of interest to be expressed as their equilibrium value (superscript "0" in what follows) plus a perturbation linearly dependent on the field (note that in equilibrium the fluid velocity is zero on the average) [14,22]:

$$\begin{aligned}
&\Psi(\boldsymbol{r},t) = \Psi^0(r) + \delta\Psi(\boldsymbol{r},t) = \Psi^0(r) + \chi(r)E\cos\theta\exp(-j\omega t)\\
&\mu_i(\boldsymbol{r},t) = \mu_i^0(r) + \delta\mu_i(\boldsymbol{r},t) = \mu_i^0(r) + \phi_i(r)E\cos\theta\exp(-j\omega t),\\
&i = 1,\ldots,N\ P(r,t) = P^0 + p(r)E\cos\theta\exp(-j\omega t)\\
&\boldsymbol{u}(\boldsymbol{r},t) = \left[-2\,\tfrac{h(r)}{r}E\cos\theta\,\hat{\boldsymbol{r}},\ \tfrac{1}{r}\tfrac{d}{dr}(rh(r))E\sin\theta\,\hat{\boldsymbol{\theta}},\ 0\,\hat{\boldsymbol{\varphi}}\right]
\end{aligned} \tag{9}$$

Here, the auxiliary functions $\chi(r)$, $\phi_i(r)$, $p(r), h(r)$ allow the transformation of the partial differential equations into a system of ordinary differential equations by substitution of the expressions into the equations (1–5), and consideration of the equations, characterizing the equilibrium (no field) situation, as detailed in the Supplementary Information file. Note that the fluid velocity components are referred to a spherical coordinate system, where the field is directed along the z axis, and θ is the angle between the field an the position vector $\mathbf{r}$.

Upon solving the mentioned system, the quantities of interest from the experimental point of view can be obtained, since the following relations can be derived for the values of the auxiliary functions on the cell limit [22]:

i. The dynamic electrophoretic mobility $u_d(\omega)$ relating the particle electrophoretic velocity to the field:

$$\begin{aligned}
&-\boldsymbol{u}|_{r\to\infty} = u_d\boldsymbol{E}\exp(-j\omega t)\\
&u_d(\omega) = \frac{2h(\omega)|_{r=b}}{b}
\end{aligned} \tag{10}$$

ii. The (complex) relative permittivity of the suspension $\varepsilon^*(\omega) = \varepsilon'(\omega) + j\varepsilon''(\omega)$, deduced in turn from the complex electrical conductivity $K^*(\omega)$:

$$\begin{aligned}
&\varepsilon'(\omega) = -\tfrac{Im[K^*(\omega)]}{\omega\varepsilon_0}\\
&\varepsilon''(\omega) = \tfrac{Re[K^*(\omega)]-\{Re[K^*(\omega)]\}_{\omega\to 0}}{\omega\varepsilon_0}\\
&K^*(\omega) = \left[\sum_{i=1}^{N}\tfrac{z_i e^2 D_i}{k_B T}n_i^0(r)\tfrac{d\phi_i}{dr}\right]_{r=b} - \sum_{i=1}^{N} z_i e n_i^0(b)\tfrac{2h(b)}{b} + j\omega\varepsilon_m\varepsilon_0\left.\tfrac{d\chi}{dr}\right|_{r=b}
\end{aligned} \tag{11}$$

A set of boundary conditions must be established for the solution of the system. The reader is referred to previous works [18], and, for the sake of conciseness, the details are provided in the Supplementary Information file. A Matlab© routine was elaborated for the resolution of the differential equations.

The main assumptions of the models described regarding the role of the polyelectrolyte coating on the electrokinetics of the particles must be pointed out. First, ions in solution are assumed to be point charges; for the case of monovalent species considered here, this assumption fails only for high concentrations. Model calculations of AC electrokinetics previously reported [23] indicate that for surface charges similar to those investigated in this work (although spread on a surface and not in a volume) and salt concentrations in the millimolar range, the effect of ion size on the

frequency response is negligible, and in any case it can only be detected at low field frequencies (below 1 kHz approximately). Note also that we have considered that the permittivity of the charged polymer layer is identical to that of the free solution; because water dipole orientation is hampered around hydrated ions, the permittivity of aqueous solutions is reduced in the persence of non-negligible ionic concentrations. Such effect is restricted to short distances (0.1–0.2 nm) from the ions, and the permittivity reaches bulk values less than 1 nm further. This is the reason why the consideration of dielectric constant lower than that of water gains importance in the inner or compact part of the double layer (the Stern layer), not considerd here, and bulk values are reasonable in the diffuse region [24]. A different issue is whether or not this condition is fulfilled inside the polymer coating. Theory and simulations on the structure of temperature-responsive microgels even in the shrunk state, have demonstrated that the assumption of constant permittivity equal to that of the medium leads to good agreement with experimental data on size and mobility of the gel particles [25,26]. Finally, concerning the analysis of particle concentration effects, the cell model is assumed to be valid. Theoretical developments by Zholskovskij et al. [27] gave a rigorous basis to the model, which has furthermore been widely used in discussing the electrokinetics of colloids, both in DC [28,29] and AC [30] electric fields. Comparison with experimental data on the dielectric dispersion of suspensions with volume concentrations up to 15 % demonstrated the validity of the cell model, even for field frequencies in excess of 1 MHz [31].

3. Experimental

3.1. Materials

All chemicals were purchased from Merck-Sigma Aldrich (Spain). Water was deionized and filtered using a Milli-Q Academic, from Millipore (France).

3.2. Methods

Silica particles were produced using the Stöber method [32,33]. Briefly, the particles were obtained by first preparing 0.5 L of solution of NH_4OH (1 mol/L), and water (3.8 mol/L) in ethanol at room temperature. Tetraethylorthosilicate or TEOS (0.17 mol/L) was added to this solution, and the final system was stirred mechanically for 2 h, always at room temperature. At the end of the process, the newly obtained suspension was centrifuged at 8000 rpm for 15 min and redispersed in water, repeating the process three times. Fig. 2 is an HRTEM picture (obtained with a Thermo Fisher Scientific (USA) TALOS F200X high-resolution transmission electron microscope) of the particles obtained. The average (±S.D.) diameter was found to be (390 ± 14) nm.

Polyelectrolyte coating by adsorption was performed by overnight stirring of a suspension of silica nanospheres (2 % concentration by volume) in a 100 mM (calculated on a monomer basis) aqueous solution of poly(styrene sulfonate), PSS, or poly(diallyl dimethyl ammonium chloride), PDADMAC, in the case of the anionic or cationic coating, respectively. The Talos microscope was used for obtaining a composition map of the coated particles surface by EDX, in order to confirm the presence of the polyelectrolytes.

Grafting of the polyelectrolytes was a more involved process. To begin with, the bare silica was activated with 4-vinylaniline radicals. In order to do so, 0.33 mL of a 37 %wt HCl aqueous solution was added to 106.75 mL of a 0.04 % wt silica aqueous suspension (4.27 g of silica). The mixture was magnetically stirred continuously all over the process. After 40 min, 0.16 g of 4-vinylaniline

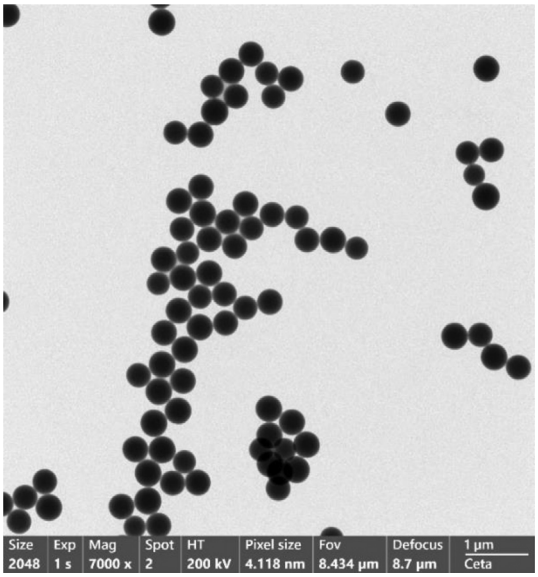

Fig. 2. HRTEM picture of the bare silica particles obtained ρ_{pol}.

was added, and the mixture was heated up to 43 °C after 10 min. Once the temperature was reached, a solution of 0.064 g of $NaNO_2$ in 10 mL of H_2O was slowly and completely added during 15 min. The product was kept at 43 °C for 16 h while stirring, then centrifuged at 20 000 rpm for 20 min. The supernatant was removed, and then acetone was added. The product was again centrifuged. The resulting activated silica was divided in two halves, using 2.135 g for the synthesis of each of the polymers (positive and negative). The used monomers were (vinylbenzyl)trimethylammonium chloride (positive), and sodium 4-vinylbenzenesulfonate as the negative one. For each polymerization, the activated silica was put into a double-necked flask fitted with a magnet and a reflux system. Next, 1.07 g of the corresponding monomer and 10.82 g of dimethyl sulfoxide (DMSO, which acts as solvent) were added. The flask with the mixture was placed into an ultrasonic bath until the product was homogenously suspended in the solvent. Then, magnetic stirring was applied all over the rest of the process. In order to initiate the polymerization, a solution of 27 mg of AIBN (Azobisisobutyronitrile) in 0.85 mL of DMSO was added to the flask. Next, the flask was set to be purged with N_2, and heated up to 70 °C after 5 min and left overnight. The resulting product was dispersed in 106 mL of ethanol after being cooled, then centrifuged at 7800 rpm for 1 h. Supernatant was removed, and the washing process was repeated twice in order to remove possible remains of the polymerization.

Hydrodynamic diameters of the coated particles were obtained by dynamic light scattering in a Zetasizer Nano-ZS from Malvern Instruments (UK). The same instrument allowed us to evaluate the DC or classical electrophoretic mobility of the particles, in order to qualitatively ascertain the modifications brought about on the surface of the particles by the different coating procedures.

The AC or dynamic mobility was determined using the electroacoustic technique [34,35] by means of Acoustosizer IIc device manufactured by Colloidal Dynamics Inc. (USA): the real and imaginary components (or the modulus and phase) of the mobility are obtained in the 1–18 MHz frequency range by analyzing the amplitude and phase of the pressure wave produced in the suspension (of arbitrary solids volume fraction) by application of an AC electric field.

The dielectric dispersion experiment sweeps a different frequency range (1 kHz to 2 MHz, roughly), but it is equally informative about the different polarization processes occuring at the

interface by the variable frequency external fields. For the determination of the dielectric dispersion (frequency dependence of the electric permittivity of the suspensions), use is made of a home-made parallel electrodes cell, built in glass. The electrodes are 1 cm radius platinum disks coated with platinum black using standard methods [36], in order to minimize the unwanted electrode polarization effect [37–39], by virtue of which the frequency dependence of the impedance of the electrode/solution interface hides the low-frequency true relaxation of the system. We used the method known as *logarithmic derivative* [40]. It involves first calculating the derivative of the raw $\varepsilon'(\omega)$ data:

$$\varepsilon_{LD}(\omega) = -\frac{\pi}{2}\frac{\partial\varepsilon'(\omega)}{\partial \ln(\omega)} \tag{12}$$

The low-frequency contribution to this quantitty is fitted to a power-law

$$\varepsilon_{LD}(\omega \to 0) = A\omega^{-m} \tag{13}$$

and subtracted from the $\varepsilon_{LD}(\omega)$ to get the polarization-corrected results:

$$\varepsilon_{LD}^{corr}(\omega) = \varepsilon_{LD}(\omega) - A\omega^{-m} \tag{14}$$

Finally, the real part of the dielectric constant is recovered by integration. The constant of integration is obtained by equating the high-frequency value of the integrated quantity to the dielectric constant of the solution (that of water in our case):

$$\varepsilon'(\omega) = -\frac{2}{\pi}\int \varepsilon\frac{corr}{LD}(\omega)\frac{d\omega}{\omega} + const. \tag{15}$$

4. Results and discussion

4.1. Particle coating

Fig. 3 shows the HRTEM appearance of the coated particles, together with their EDX composition maps. Although the drying process needed in ordinary TEM does alter the nanostructure, the pictures in Fig. 3 allow to distinguish roughly between the two kinds of particle treatments. The grafted chains tend to produce fused particles upon drying, with a bridge clearly observable between neighbors. In the case of the soft coating, one can observe that several particles tend to be bound. The composition maps confirm the presence of the two polyelectrolytes on the respective particles, through detection of sodium and sulfur in the case of the anionic polyelectrolyte (either PSS or poly(sodium 4-vinylbenzene sulfonate)), and of nitrogen and chlorine when the coating is cationic (PDADMAC or poly(vinylbenzyl trimethylammonium chloride)). Dynamic light scattering measurements yield similar hydrodynamic diameters for bare silica (406 ± 5 nm), and for anionic (adsorbed: 419 ± 52 nm; grafted: 412 ± 13 nm) and cationic layers (417 ± 4 nm). Interestingly enough, the value obtained for grafted cationic polymer is sensibly larger, namely, 596 ± 5 nm, a fact that we interpret as a more effective and open coating in this case. This was really expected, considering the likely radial disposition of the polymer chains and the overall positive attraction with the negatively charged (see below) silica core.

4.2. Overall interfacial charge

An indirect way to confirm the coating consists of determining the electrophoretic mobility of the coated particles and compare it to that of the bare silica spheres. Although, as mentioned, such an evaluation lacks information about the nanostructure details, at least it will provide a sort of overview of the interfacial changes produced by the treatment. Fig. 4 contains that information. The mobility is plotted as a function of KCl concentration for both silica cores and polyelectrolyte-coated particles. Note that silica is negative as expected, its mobility increasing slightly between 0.1 mM and 1 mM KCl, a suggestion of finite conductivity in the Stern layer [35] that will not be further studied in the present work. More significant is the demonstration of the coatings: the charge remains negative upon anionic polyelectrolyte coverage whereas it changes to positive with cationic polyelectrolyte shell. No important differences are observed between both types of coating, and this is the rather limited information that standard electrophoresis can provide. This is in striking contrast with the AC electrokinetic results to be described below.

4.3. Model predictions for AC electrokinetics

Although, as mentioned, results are available on the electrokinetics in AC fields for both adsorbed [15,41,42] and grafted [21,43] polyelectrolyte layers, no comparison between both

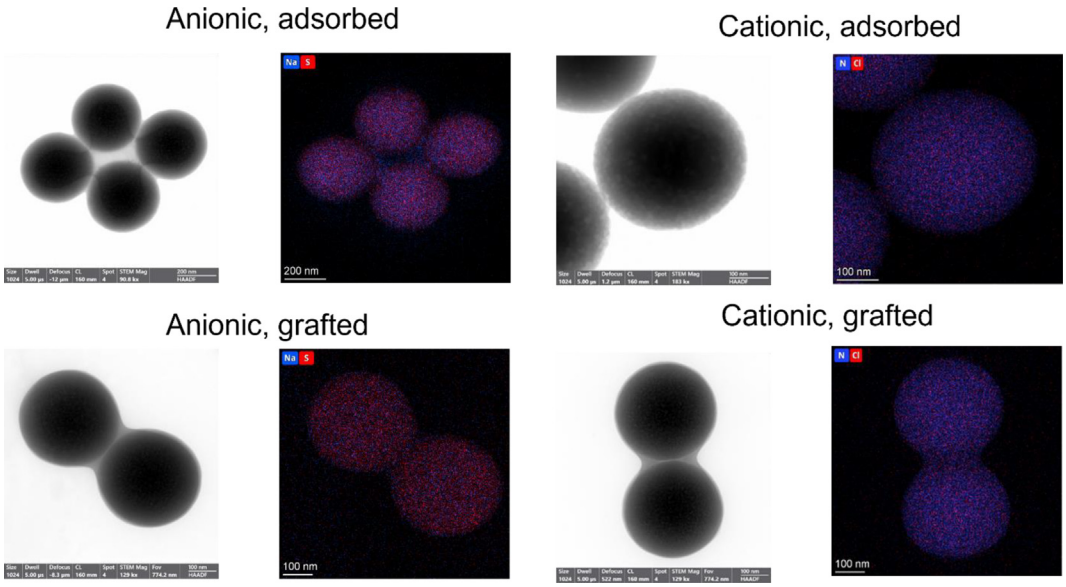

Fig. 3. HRTEM pictures and EDX composition maps of the polyelectrolyte coated particles.

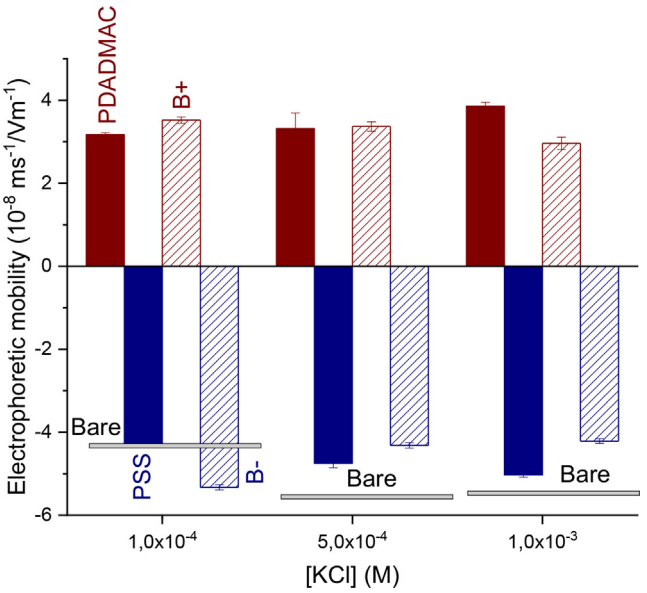

Fig. 4. Electrophoretic mobility of bare (grey horizontal lines) and coated (full bars: adsorbed; patterned bars: grafted) silica particles. PSS (PDADMAC): adsorbed anionic (cationic) polymer; B- (B +): grafted or brush-like anionic (cationic) chains.

approaches has ever been presented in the past. In the following we will show some representative results.

Fig. 5 shows the frequency dependences of the real parts of the dynamic mobility and the dielectric constant of soft and grafted coated particles. Note first to what extent the information provided by dynamic mobility completes that obtained from the dielectric spectra, regarding the frequency ranges swept in each case. The latter shows a very pronounced decrease for frequencies around 10^4-10^5 rad/s. This decline is the manifestation of the $\alpha-$ or *polarization* relaxation [44,45]: for such frequencies, the field changes too rapidly for the concentration polarization clouds to develop. As a result, the out-of-phase currents associated to diffusion fluxes disappear, and the permittivity shows a reduction. Such pronounced effect translates into just a tiny (if any) decrease in the mobility. The $\alpha-$ relaxation is greatly magnified in the case of the brush structure, and much smaller for just adsorbed layers. In contrast, a feature is shown by dynamic mobility in the vicinity of 10 Mrad/s, not appreciable at all in the permittivity spectrum. It consists of a significant increase of the mobility (in absolute value), which is associated to a decrease in the dipole moment because of the well-known Maxwell-Wagner or Maxwell-Wagner-O'Konski (MW or MWO) electric double layer relaxation. The mobility jump is again much more appreciable in the case of brush layers.

Finally, for the highest field frequency, the mobility goes to zero, in a process known as *inertial* relaxation, strongly dependent on the particle size and the medium viscosity. If such frequency is reached, the field changes direction too fast for allowing any motion of the fluid or the particles, and the electrophoresis displacement vanishes [46]. We conclude that the nanostructure of the polyelectrolyte layer greatly affects the AC electrokinetics of coated particles, and in fact it captures a number of aspects that are invisible by other methods.

4.4. The AC electrokinetics of bare silica

With the aim of establishing a comparison between the electrokinetic behaviours of bare and treated particles, we consider first that of the cores. Fig. 6 contains data on the dynamic mobility (again, for brevity only the real part is considered) and the dielectric dispersion of silica spheres for two volume fractions of solids

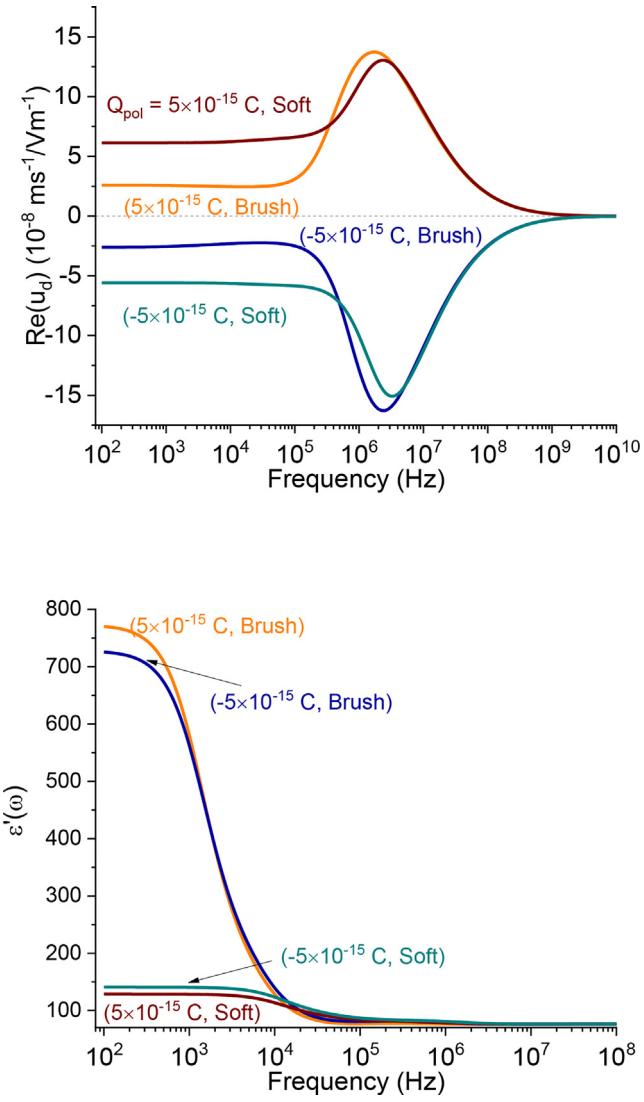

Fig. 5. Real part of the dynamic mobility (*top*) and of the dielectric constant (*bottom*) for adsorbed (Soft) and grafted (Brush) layers of polyelectrolyte, both cationic (positive Q_{pol}) and anionic (negative Q_{pol}). The core is negatively charged with -1.2×10^{-15} C total charge, and its radius is 200 nm. For all layers, the thickness is 30 nm, and the friction parameter is $\lambda R_C = 1$.

(2 % and 4 %) and two concentrations of KCl (0.1 mM and 0.5 mM). Let first point out that the mobility data display little structure, as only the inertial relaxation (tendency to zero) is clearly observable, hiding the MW relaxation. The only exception seems to be the 0.1 mM, 2 % volume fraction suspensions, which in any case display a very weak increase in mobility. On the other hand, in all cases and frequencies, the mobility increases with ionic strength for the values tested (recall the DC mobility data in Fig. 4). This relatively limited information is in contrast with that extracted from the dielectric spectra behavior: the most striking observation in these data is the appreciable *alpha* or concentration polarization relaxation, to which a decrease can be associated, larger for higher particle volume fractions and ionic strengths, as found in suspension dielectric models [31].

4.5. Adsorbed vs Grafted layers: Dynamic mobility and dielectric spectra

Next, we analyze the effect on the electrokinetic properties just described of coating with the anionic or cationic polyelectrolyte

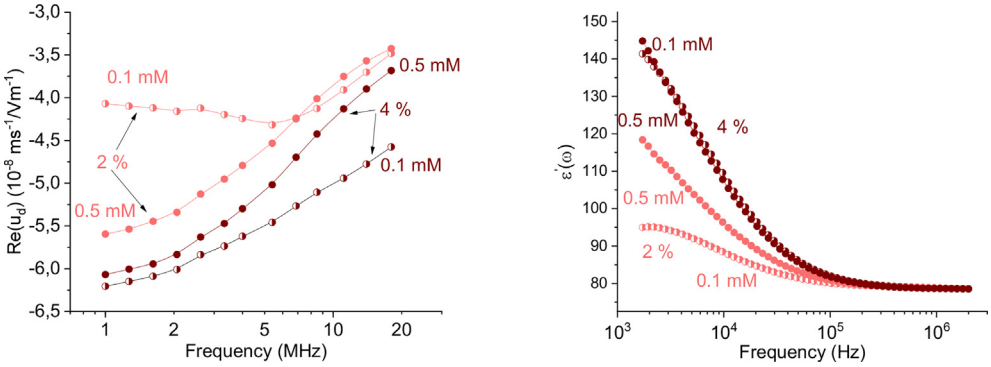

Fig. 6. Experimental values of the real components of the dynamic mobility (left) and the dielectric constant (right) of silica suspensions for the particle volume fractions (in %) and the KCl concentrations (mM) indicated.

using the two methods. Fig. 7 shows the dynamic mobility data. A significant MW elevation of the mobility is observed when the coating is brush-like (grafted); in contrast, the adsorbed layer structure leads to simple inertial decrease. It is suggested that the polyelectrolyte brush protects the particles more efficiently against aggregation: consequently, the average size will remain almost identical to that of the individual particles, and the inertia will be displaced towards higher frequencies. The effect is more appreciable when the polyelectrolyte is cationic (panels c, d vs a, b), as one expects from a better binding favoured by electrostatics. The monotonous mobility decrease observed for soft coatings can be justified by a lower overall charge of the layer and a subsequent tendency of the particles to form aggregates: both effects will mask the possible MW rise by the reduced surface conductivity and/or the appearance of inertia decrease for lower frequencies, due to the larger average particle size. Both phenomena seem to be absent in the case of the positive brush layer, clear evidence of the efficient and highly charged coating achieved in such situation. This can be confirmed by the analysis of the alpha relaxation in dielectric spectra, as will be discussed below.

Figs. 8 and 9 contain the results pertaining to the dielectric spectra of the suspensions. The position of the maximum in the log derivative $\varepsilon_{LD}(\omega)$ gives us a clear indication of particle size in the suspensions. Thus, the frequency of such maximum is found to be higher in the case of the brush-like coating, indicating a smaller average diameter. Note, however, that $\varepsilon_{LD}(\omega)$ for brush (+) par-

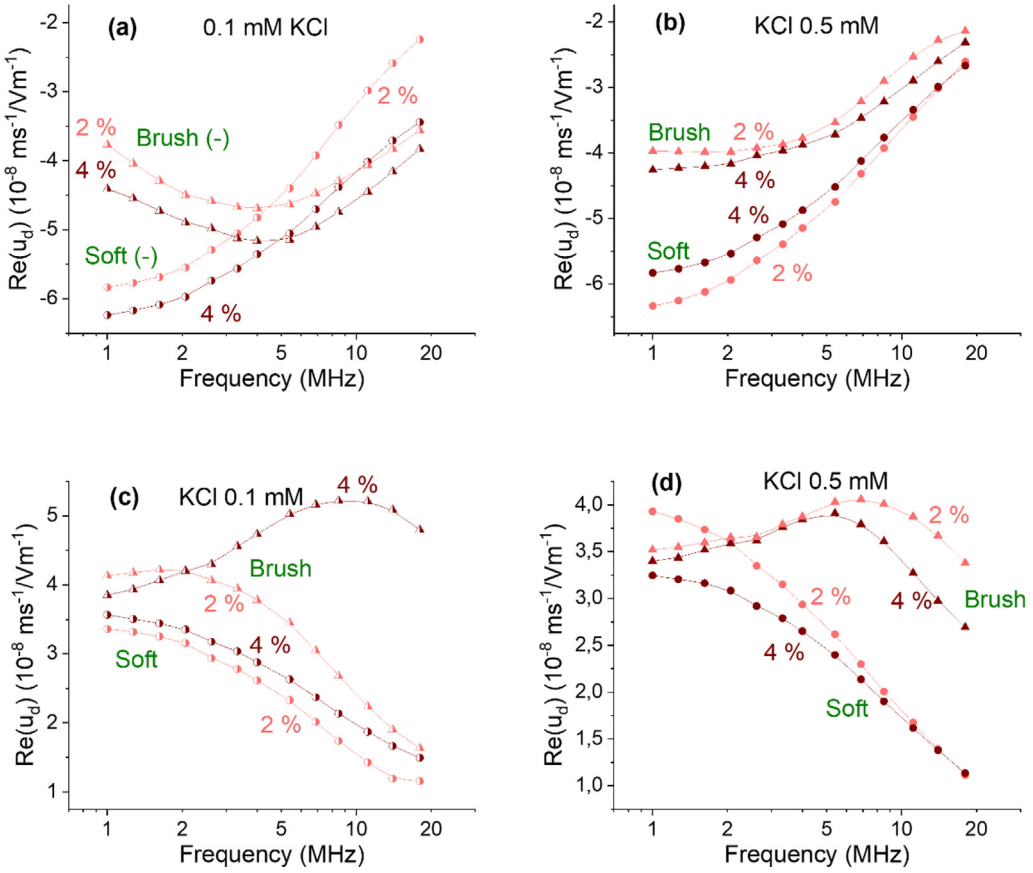

Fig. 7. Real part of the dynamic mobility of polyelectrolyte-coated silica. (a,b): anionic, adsorbed or grafted, with volume fractions 2 % and 4 %, and KCl concentrations 0.1 mM (a) and 0.5 mM (b). (c,d): same as (a,b), but for cationic polymer.

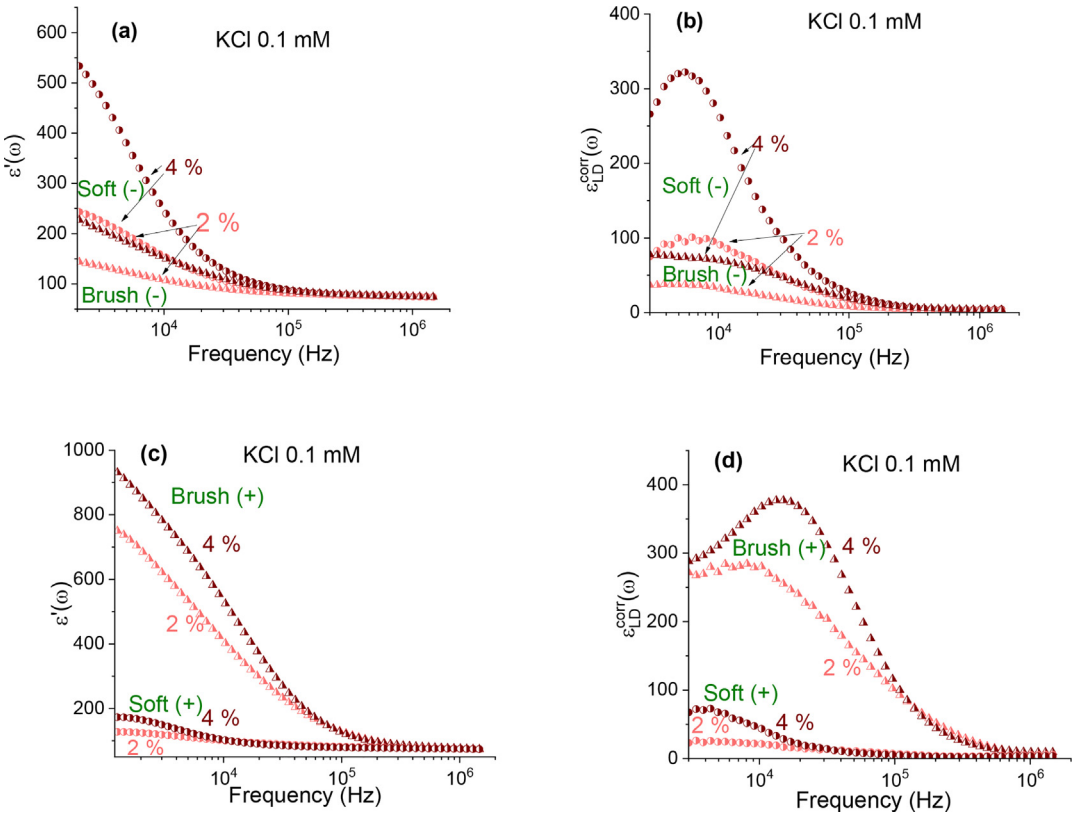

Fig. 8. Real part (left column) and its logarithmic derivative (right column) of the relative permittivity of polyelectrolyte-coated silica. Negative polymer: a,b; positive polymer: c,d. 0.1 mM KCl solution in all cases.

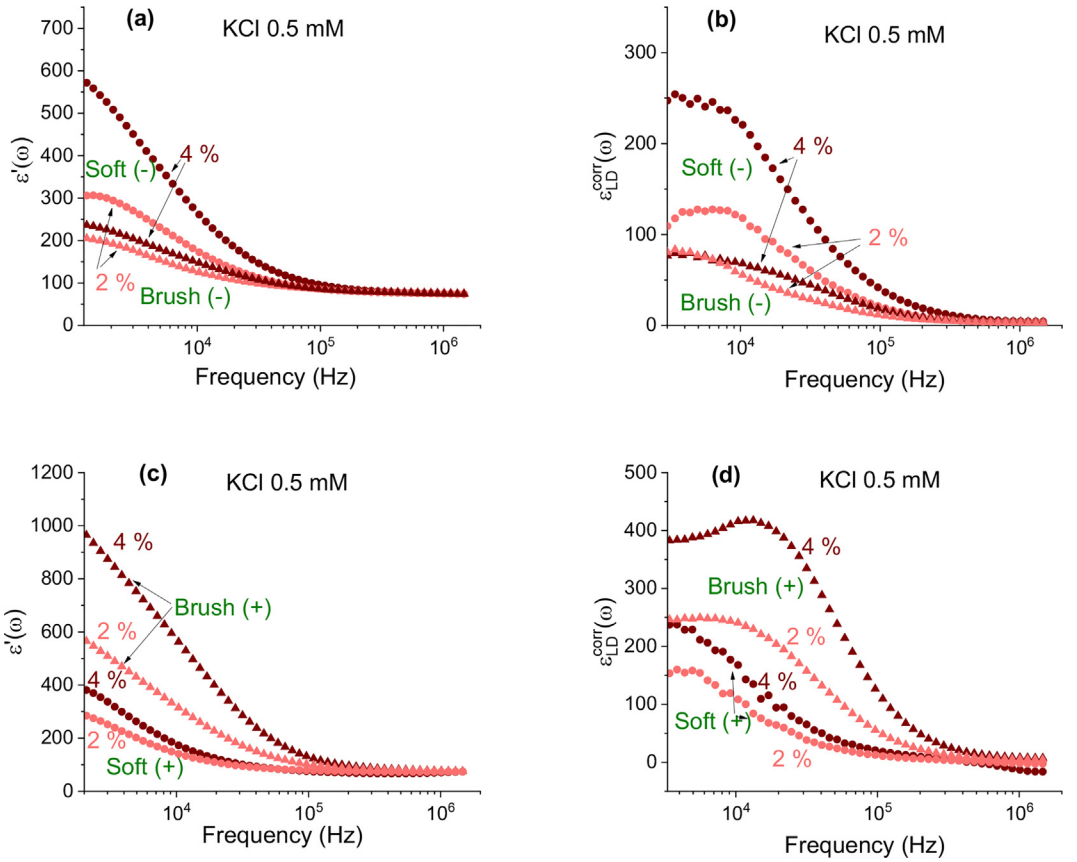

Fig. 9. Same as Fig. 8, but for 0.5 mM KCl.

ticles suggests a low-frequency elevation that can be associated to the existence of aggregates (larger average size, lower $\alpha-$ relaxation frequency). In contrast, the soft coating leads directly to a low-frequency maximum, and this suggests that individual particles are much less abundant than aggregates. As observed, $\varepsilon'(\omega)$ data are not so sensitive to these aggregation processes, and their existence is rather manifested as a wider relaxation. The latter data are however useful as indicators of the overall charge, as the amplitude of the relaxation is correlated with interfacial charge. Hence, from Fig. 8a,c and 9a,c we can conclude that the charge of the (+) brush coating is much larger than that of the negative one. Also, the partial compensation of the negative silica charge and the positive charge of the soft cationic layer leads to a reduced relaxation amplitude (Fig. 8c,9c), as compared to that of the negative soft layer (Fig. 8a, 9a). No such effect is observed when the coating is brush-like, as the layer extends so much from the surface that its charge becomes dominant.

Regarding the variation with KCl concentration of the behaviour described, comparison of Figs. 8 and 9 allows us to conclude that the qualitative dependences are very similar for both ionic strengths, and, as expected from the theory of dielectric dispersion of suspensions [47], the larger concentration of ions enriches the polarization clouds and give rise to an increase in the dielectric decrement around the α-relaxation for 0.5 mM KCl as compared to 0.1 mM. A similar effect occurs when it is the particle concentration that is increased [31], as long as the volume fraction of solids is not too high as to reduce the polarization clouds of neighbor particles.

4.6. Comparison with model predictions

For the sake of brevity, only some cases will be considered regarding the performance of the model described in explaining the experimental data. The fitting strategy included to obtain the best-fit parameters from the (better-defined) mobility results and using the thus obtained parameters for predicting the dielectric relaxation. A minimization of the relative sum of squares of differences between predicted and measured values was used as best-fit criterion. It must be considered that the simultaneous fitting of two sets of data covering separate frequency ranges is in this case hampered by the already mentioned polydispersity of the suspensions brought about by possible formation of structures mediated

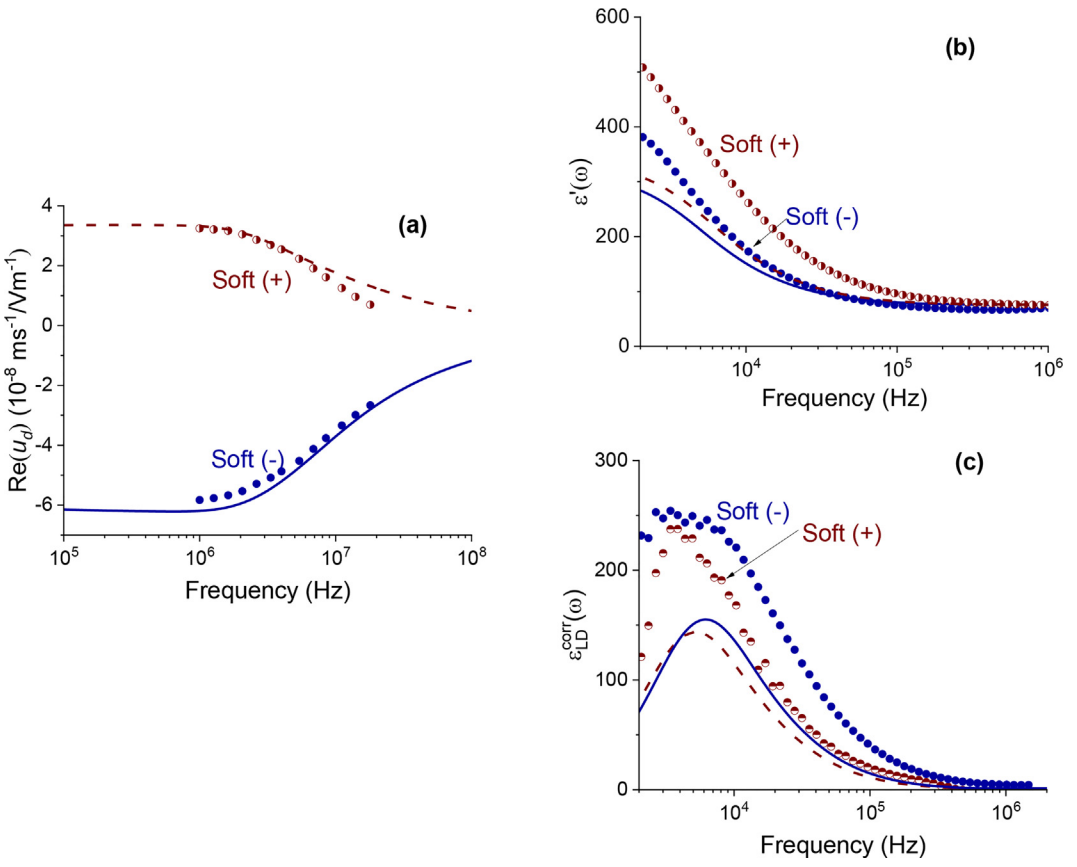

Fig. 10. Experimental (data points) and calculated (lines) frequency dependences of the real part of the dynamic mobility (a) and the dielectric constant (ε': b; ε_{LD}^{corr}: c) of 2 % suspensions of silica spheres coated by a soft (adsorbed) layer of anionic or cationic polyelectrolytes. KCl concentration: 0.5 Mm.

Table 1
Best-fit parameters used for the theoretical predictions displayed in Fig. 11, 12.

Sample	Core radius, R_c (nm)	Layer thickness, L (nm)	Friction parameter*, λ (nm^{-1})	Total charge of the polymer layer, Q_{pol} (10^{-14}C)
Soft (+)	400	30	0.18	+4.0
Soft (-)	370	30	0.09	−3.0
Brush (+)	180	70	1.67	+1.2
Brush (-)	200	100	0.51	−0.2

*Corresponds to the surface value, λ_0 (Eq. (8)) in the case of brush structures.

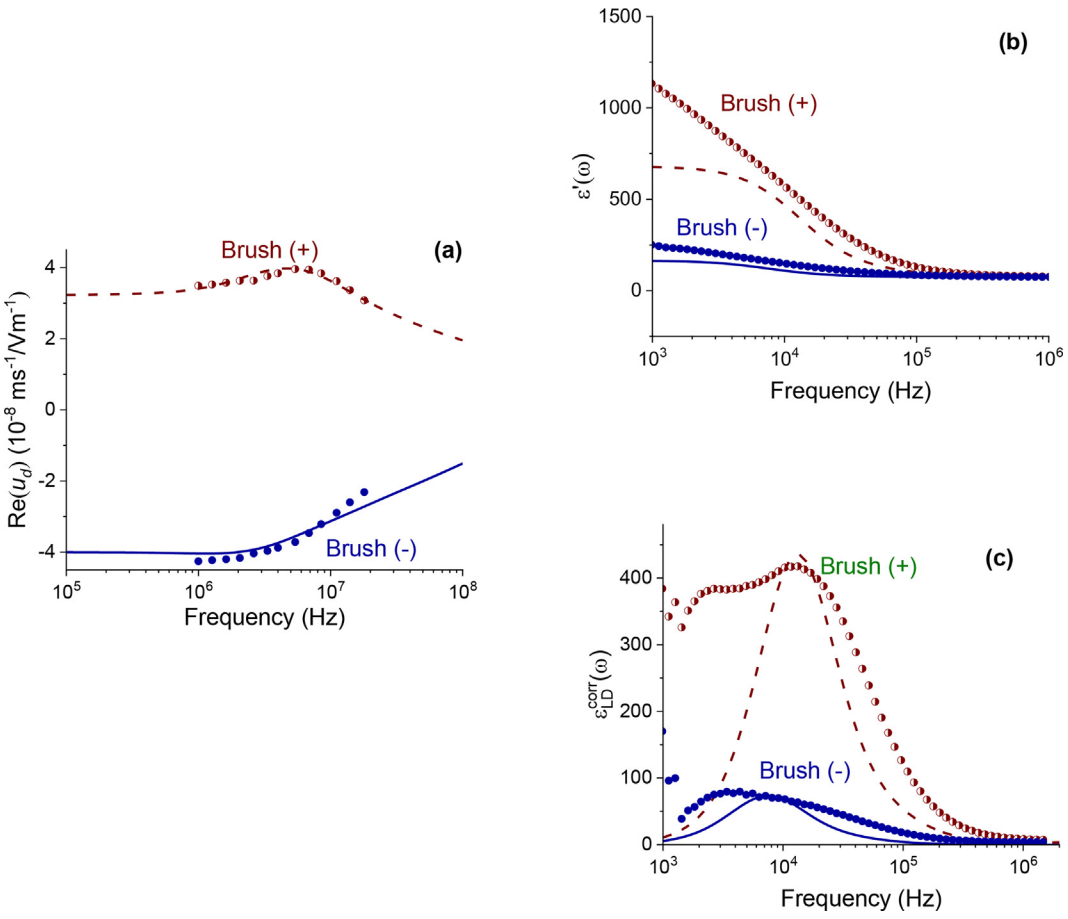

Fig. 11. Same as Fig. 10, but for grafted polyelectrolytes.

by the polymer chains. It is worth mentioning that the calculations of $\varepsilon'(\omega)$ tend to overestimate the experimental data. This is a well-known feature of dielectric dispersion modelling, as the complete elimination of electrode polarization cannot be guaranteed [39] by any method, and, furthermore, polarization mechanisms other than those associated to the ionic atmosphere have not been considered in the model. It is in these complex systems that the proposed ac electrokinetic techniques show their power in explaining and predicting the colloidal behavior of the suspensions, as discussed below.

Fig. 10 shows the measured and predicted values of the two quantities of interest when the coating layer is adsorbed (soft). Note the goodness of fit (best in the case of the mobility, as mentioned) for very reasonable values of the model parameters (Table 1). Let us point out that the core radius R_C used for fitting is larger than that measured for bare particles (Fig. 2), confirming our hypothesis that the adsorbed layer engulfs more than one particle (Fig. 3). The adsorbed layers show a high charge (comparable in absolute values for the two polymers), and they are relatively thin both for the positive and negative polyelectrolytes. Its resulting compact structure justifies the relatively high values of the friction parameter λR_c estimated from the fittings.

Regarding the brush-like coating (Fig. 11), the goodness of fit is equally significant for both quantities. Note that the model explains very well the MW elevation of the mobility (Fig. 11a) and the huge dielectric relaxation amplitude attained with the positive coating (Fig. 11b), a manifestation of the presence of the extended and highly charged structure of the polyelectrolyte layer. The wide $\varepsilon'(\omega)$ relaxation and the suggested low-frequency peak of the logarithmic derivative $\varepsilon_{LD}^{corr}(\omega)$ cannot be captured by the model, as this considers monodisperse suspensions with the size of single particles. This confirms, as mentioned above, that such features of the dielectric spectra are associated to the formation of aggregates (probably dimers, see Fig. 3) bound by the polymer chains of adjacent particles. These effects are not so clearly apparent in the case of soft coatings, an indication of the fact that the ac response is dominated in these systems by the aggregates: although they will coexist with individual particles, the contribution of the latter is not so appreciable because of the limited extension of the coating layer.

In the case of negative polyelectrolyte coatings, similar facts are observable regarding the width of the dielectric relaxation and the presence of two peaks (note the shoulders in $\varepsilon_{LD}^{corr}(\omega)$) in Fig. 11b,c, although they are weaker because of the smaller charge of the negative brush (Table 1).

5. Conclusions

The electrokinetic study described in this paper demonstrates that dynamic electrophoretic mobility and dielectric constant of suspensions, determined as a function of the frequency of the AC external field, can provide worth a lot of information on the nanostructure of coated particles. Furthermore, a clear distinction can be established between charged polymer layers adsorbed on the particles in the form a soft, rather compact layer, and polymers grafted on the particles upon growing of the monomers in a brush-like fashion. This is because, as demonstrated with the model elaborated to that aim, the electrokinetic behaviour (AC electrophoresis and dielectric dispersion) differs significantly for both types of

coatings. Simple dc electrophoresis does not allow to distinguish such features, as AC fields disclose much wider information. Experiments performed on suspensions of silica particles coated by either cationic or anionic (soft and brush-like), demonstrate that, in general, a grafted layer magnifies the electrokinetic response. The fact that the friction experienced by the ions decreases when increasing the distance to the core can explain this. The model elaborated for both cases, and different volume fractions of solids and ionic concentrations explains most of the experimental tendencies and provides reasonable values for the parameters characterizing the nanostructure in the unperturbed state in suspension.

CRediT authorship contribution statement

S. Ahualli: Conceptualization, Funding acquisition, Software, Writing – review & editing. **S. Orozco-Barrera:** Data curation, Investigation. **A.L. Medina Castillo:** Data curation, Investigation. **A.V. Delgado:** Conceptualization, Supervision, Writing – original draft.

Data availability

Data available in the following address: https://figshare.com/articles/dataset/Effect_of_coating_nanostructure_on_the_electrokinetics_of_polyelectrolyte-coated_particles_Grafted_vs_adsorbed_polymer/22015811

Declaration of Competing Interest

The authors declare that they have no known competing financial interests or personal relationships that could have appeared to influence the work reported in this paper.

Acknowledgements

Financial support from FEDER/Junta de Andalucía-Consejería de Transformación Económica, Industria, Conocimiento y Universidades, Project PI20-00233, Proyectos I + D + i, Programa Operativo FEDER Andalucía 2014-2020 (Project A.FQM.492.UGR20), and Project (TED2021-131855B-I00), financed/supported by: ERDF/Ministry of Science and Innovation-State Research Agency is gratefully acknowledged. Funding for open access charge: Universidad de Granada / CBUA.

References

[1] A.V. Delgado, J.L. Viota, M.M. Ramos-Tejada, J.L. Arias, Particle geometry, charge, and wettability: The fate of nanoparticle-based drug vehicles, in: H. Ohshima, K. Makino (Eds.), Colloid and interface Science in Pharmaceutical Research and Development, Elsevier, Amsterdam, The Netherlands, 2014, pp. 443–467.
[2] R.A. Petros, J.M. DeSimone, Strategies in the design of nanoparticles for therapeutic applications, Nat. Rev. Drug Disc. 9 (8) (2010) 615–627.
[3] M.A. Dobrovolskaia, S.E. McNeil, Immunological properties of engineered nanomaterials, Nat. Nanotechnol. 2 (8) (2007) 469–478.
[4] M.A. Dobrovolskaia, P. Aggarwal, J.B. Hall, S.E. McNeil, Preclinical studies to understand nanoparticle interaction with the immune system and its potential effects on nanoparticle biodistribution, Mol. Pharmaceutics. 5 (4) (2007) 487–495.
[5] D.A. Hume, The mononuclear phagocyte system, Curr. Opin. Immunol. 18 (1) (2006) 49–53.
[6] M.D. Howard, M. Jay, T.D. Dziublal, X. Lu, PEGylation of nanocarrier drug delivery systems: state of the art, J. Biomed. Nanotechnol. 4 (2) (2008) 133–148.
[7] J. Deng, J. He, J.S. Zheng, S. Terakawa, H. Huang, L.C. Fang, Y. Li, P. Cheng, L.L. Jiang, Preparation and application of amino-and dextran-modified superparamagnetic iron oxide nanoparticles, Part. Sci. Technol. 31 (3) (2013) 241–247.
[8] A. Gulbake, S.K. Jain, Chitosan: a potential polymer for colon-specific drug delivery system, Expert Opin. Drug Deliv. 9 (6) (2012) 713–729.
[9] J. Meadows, P.A. Williams, M.J. Garvey, R. Harrop, Manipulation of the stability and redispersibility of polyelectrolyte-coated latex particles in various electrolyte solutions, J. Colloid Interface Sci. 148 (1) (1992) 160–166.
[10] C.N. Likos, Soft matter with soft particles, Soft Matter 2 (6) (2006) 478–498.
[11] H. Ohshima, Theory of electrostatics and electrokinetics of soft particles, Sci. Technol. Adv. Mater. 10 (6) (2009).
[12] G. Decher, J.D. Hong, J. Schmitt, Buildup of ultrathin multilayer films by a self-assembly process: III, Consecutively alternating adsorption of anionic and cationic polyelectrolytes on charged surfaces, Thin Solid Films. 210 (1992) 831–835.
[13] G. Decher, Fuzzy nanoassemblies: toward layered polymeric multicomposites, Science 277 (5330) (1997) 1232–1237.
[14] S. Ahualli, M.L. Jimenez, F. Carrique, A.V. Delgado, AC electrokinetics of concentrated suspensions of soft particles, Langmuir 25 (4) (2009) 1986–1997.
[15] J.F. Duval, H. Ohshima, Electrophoresis of diffuse soft particles, Langmuir 22 (8) (2006) 3533–3546.
[16] J.F. Duval, F. Gaboriaud, Progress in electrohydrodynamics of soft microbial particle interphases, Curr. Opin. Colloid Interface Sci. 15 (3) (2010) 184–195.
[17] H. Ohshima, Electrophoretic mobility of soft particles, J. Colloid Interface Sci. 163 (2) (1994) 474–483.
[18] S. Ahualli, S. Bermudez, F. Carrique, M.L. Jimenez, A.V. Delgado, AC Electrokinetics of Salt-Free Multilayered Polymer-Grafted Particles, Polymers 12 (9) (2020) 2097.
[19] M.M. Ramos-Tejada, J.L. Viota, K. Rudzka, A.V. Delgado, Preparation of multifunctionalized Fe3O4/Au nanoparticles for medical purposes, Colloids Surf. 128 (2015) 1–7.
[20] M.L. Jimenez, A. V. Delgado AV, S. Ahualli, M. Hoffmann, A. Witteman, M. Ballauff,, Giant permittivity and dynamic mobility observed for spherical polyelectrolyte brushes, Soft Matter 7 (8) (2011) 3758–3762.
[21] S. Ahualli, M. Ballauff, F.J. Arroyo, A.V. Delgado, M.L. Jimenez, Electrophoresis and dielectric dispersion of spherical polyelectrolyte brushes, Langmuir 28 (47) (2012) 16372–16381.
[22] H. Ohshima, Dynamic electrophoretic mobility of spherical colloidal particles in concentrated suspensions, J. Colloid Interface Sci. 195 (1) (1997) 137–148.
[23] M.J. Aranda-Rascón, C. Grosse, J.J. López-García, J. Horno, Influence of the finite ion size on the predictions of the standard electrokinetic model: Frequency response, J. Colloid Interface Sci. 336 (2) (2009) 857–864.
[24] J. Lyklema, Wetting, in J. Lyklema (Ed.), Fundamentals of Interface and Colloid Science Volume I: Fundamentals, Academic Press, London, 1991, 5.1-5.105.
[25] S. Ahualli, J.A. Maroto-Centeno, A. Pikabea, J. Forcada, M. Quesada-Pérez, Coarse-grained simulation study of dual-stimuli-responsive nanogels, Colloid Polym. Sci. 294 (4) (2016) 735–741.
[26] I. Adroher-Benitez, S. Ahualli, D. Bastos-Gonzalez, J. Ramos, J. Forcada, A. Moncho-Jorda, The effect of electrosteric interactions on the effective charge of thermoresponsive ionic microgels: Theory and experiments, J. Polymer Sci. Part B: Polymer Physics. 54 (20) (2016) 2038–2049.
[27] E.K. Zholkovskij, J.H. Masliyah, V.N. Shilov, S. Bhattacharjee, Electrokinetic phenomena in concentrated disperse systems: general problem formulation and spherical cell approach, Adv. Colloid Interface Sci. 134 (2007) 279–321.
[28] W.L. Chen, H.J. Keh, Electroosmosis and Electric Conduction of Electrolyte Solutions in Charge-Regulating Fibrous Media, Colloids and Interfaces. 5 (1) (2021) 19.
[29] S.K. Maurya, P.P. Gopmandal, S. De, H. Ohshima, S. Sarkar, Electrokinetics of Concentrated Suspension of Soft Particles with pH-Regulated Volumetric Charges, Langmuir 37 (2) (2021) 703–712.
[30] J.J. López-García, C. Grosse, J. Horno, Numerical calculation of the electrophoretic mobility of concentrated suspensions of soft particles, J. Colloid and Interface Sci. 301 (2) (2006) 651–659.
[31] F. Carrique, F.J. Arroyo, M.L. Jimenez, A.V. Delgado, Dielectric response of concentrated colloidal suspensions, J. Chem. Phys. 118 (4) (2003) 1945–1956.
[32] W. Stöber, A. Fink, E. Bohn, Controlled growth of monodisperse silica spheres in the micron size range, J. Colloid Interface Sci. 26 (1) (1968) 62–69.
[33] G.H. Bogush, M.A. Tracy, C.F. Zukoski, Preparation of monodisperse silica particles: control of size and mass fraction, J. Non-Cryst. Solids. 104 (1) (1988) 95–106.
[34] R.J. Hunter, Changes in the zeta potential of colloidal titanium dioxide after exposure to a radio frequency electric field using a circulating sample, Colloids Surf. A. 141 (1) (1998) 37–66.
[35] A.V. Delgado, F. Gonzalez-Caballero, R.J. Hunter, L.K. Koopal, J. Lyklema, Measurement and interpretation of electrokinetic phenomena, J. Colloid Interface Sci. 308 (2) (2007) 194–224.
[36] M.C. Tirado, F.J. Arroyo, A.V. Delgado, C. Grosse, Measurement of the low-frequency dielectric properties of colloidal suspensions: comparison between different methods, J. Colloid Interface Sci. 227 (1) (2000) 141–146.
[37] H.P. Schwan, Electrode polarization impedance and measurements in biological materials, Ann. N.Y. Acad. Sci. 148 (1) (1968) 191–209.
[38] P.J. Beltramo, E.M. Furst, A simple, single-measurement methodology to account for electrode polarization in the dielectric spectra of colloidal dispersions, Chem. Lett. 41 (10) (2012) 1116–1118.
[39] C. Chassagne, E. Dubois, M.L. Jimenez, J.M. Van Der Ploeg, J. Van Turnhout, Compensating for electrode polarization in dielectric spectroscopy studies of colloidal suspensions: theoretical assessment of existing methods, Front. Chem. 4 (2016) 30.
[40] M.L. Jimenez, F.J. Arroyo, J. Van Turnhout, A.V. Delgado, Analysis of the dielectric permittivity of suspensions by means of the logarithmic derivative of its real part, J. Colloid Interface Sci. 249 (2) (2002) 327–335.

[41] A.V. Delgado, F. Carrique, M.L. Jimenez, S. Ahualli, F.J. Arroyo, Electrokinetics of Concentrated Colloidal Dispersions, in: S.P. Stoylov, M.V. Stomienova (Eds.), Molecular and Colloidal Electro-Optics (Surfactant Science Book 134), CRC Press, 2007, pp. 149–192.
[42] J.F. Duval, C. Werner, R. Zimmermann, Electrokinetics of soft polymeric interphases with layered distribution of anionic and cationic charges, Curr. Opin. Colloid Interface Sci. 24 (2016) 1–12.
[43] J.R. Martin, I. Bihannic, C. Santos, J.P.S. Farinha, B. Deme, F.A. Leermakers, J.P. Pinheiro, E. Rotureau, J.F. Duval, Structure of multiresponsive brush-decorated nanoparticles: a combined electrokinetic, DLS, and SANS study, Langmuir. 31 (16) (2015) 4779–4790.
[44] S.S. Dukhin, V.N. Shilov, Dielectric phenomena and the double layer in disperse systems and polyelectrolytes, Jerusalem Keter Publishing, 1974.
[45] V.N. Shilov, A.V. Delgado, F. Gonzalez-Caballero, J. Horno, J.J. Lopez-Garcia, C. Grosse, Polarization of the electrical double layer. Time evolution after application of an electric field, J. Colloid Interface Sci. 232 (1) (2000) 141–148.
[46] R.W. O'Brien, D.W. Cannon, W.N. Rowlands, Electroacoustic determination of particle size and zeta potential, J. Colloid Interface Sci. 173 (2) (1995) 406–418.
[47] S. Ahualli, M.L. Jimenez, A.V. Delgado, F.J. Arroyo, F. Carrique, Electroacoustic and dielectric dispersion of concentrated colloidal suspensions, IEEE Trans. Diel. Electr. Insulat. 13 (3) (2006) 657–663.